Journal of Global Antimicrobial Resistance 19 (2019) 255–261

Contents lists available at ScienceDirect

Journal of Global Antimicrobial Resistance

journal homepage: www.elsevier.com/locate/jgar

Efficacy of newly isolated and highly potent bacteriophages in a mouse model of extensively drug-resistant *Acinetobacter baumannii* bacteraemia

Lika Leshkasheli[a], Mzia Kutateladze[a], Nana Balarjishvili[a], Darejan Bolkvadze[a], Jonathan Save[b], Frank Oechslin[b,c], Yok-Ai Que[d], Grégory Resch[b,*]

[a] *The Eliava Institute of Bacteriophages, Microbiology and Virology, Tbilissi, Georgia*
[b] *Department of Fundamental Microbiology, University of Lausanne, Switzerland*
[c] *Department of Biochemistry, Microbiology and Bio-Informatic, University Laval, Québec, Canada*
[d] *Department of Intensive Medicine, Inselspital, Bern, Switzerland*

ARTICLE INFO

Article history:
Received 5 March 2019
Received in revised form 15 April 2019
Accepted 6 May 2019
Available online 14 May 2019

Keywords:
Bacteriophage
Phage therapy
Bacteraemia
Sepsis
Extensively drug-resistant *A. baumannii* (XDRAB)
Multidrug-resistant *A. baumannii* (MDRAB)

ABSTRACT

Objectives: Bacteraemia can be caused by *Acinetobacter baumannii* (*A. baumannii*), with clinical manifestations ranging from transient bacteraemia to septic shock. Extensively drug-resistant *A. baumannii* (XDRAB) strains producing the New Delhi metallo-ß-lactamase, which confers resistance to all ß-lactams including carbapenems, have emerged. Infected patients suffer increased mortality, morbidity and length of hospitalisation. The lack of new antimicrobials has led to a renewed interest in phage therapy, the so-called forgotten cure. Accordingly, we tested new lytic bacteriophages in a *Galleria mellonella* and a mouse model of XDRAB-induced bacteraemia.

Methods: Galleria mellonella were challenged with 5.10^5 CFU of the XDRAB strain FER. Phages vB_AbaM_3054 and vB_AbaM_3090 were administrated alone or in combination 30 min after bacterial challenge. Saline and imipenem were injected as controls. Mice were intraperitoneally (i.p.) challenged with 6.10^7 CFU of *A. baumannii* FER. vB_AbaM_3054 and vB_AbaM_3090 were administrated i.p. alone or in combination 2 h after bacterial challenge. Saline and imipenem were injected as controls. Larvae and mice survival were followed for 7 days and compared with Log-Rank (Mantel-Cox) and Gehan-Breslow-Wilcoxon tests.

Results: Phage-based treatments showed high efficacy in larvae (ca. 100% survival at 80 h) and mice (ca. 100% survival at day 7) compared with the untreated controls (0% survival at 48 h and 24 h in larvae and mice, respectively).

Conclusions: The present data reporting efficacy of phage therapy in a mouse model of bacteraemia support the development of phage-based drugs to manage infection due to multi-drug resistant *A. baumannii* and particularly XDRAB.

1. Introduction

Despite being naturally present on human skin [1], the aerobic Gram-negative bacterium *Acinetobacter baumannii* (*A. baumannii*) is associated with major outbreaks of nosocomial infections, especially in severely ill patients hospitalised in intensive care units (ICUs) [2]. It produces various types of infections such as bacteraemia, pneumonia, endocarditis, meningitis and skin, soft-tissue and urinary tract infections. In view of its extraordinary capacity to escape currently available antibiotics, it has been classified amongst the ESKAPE pathogens (*Enterococcus faecium, Staphylococcus aureus, Klebsellia pneumoniae*), *A. baumannii*, and *Enterobacter* spp.) [3,4]. Infectious disease specialists consider this bacterium as an emerging threat more worrying than methicillin-resistant *S. aureus* (MRSA). A recent study involving 27 ICUs from nine European countries listed it as the third most common pathogen encountered in patients admitted with or having developed nosocomial pneumonia [5]. Tigecycline, the first representative of the new glycylcycline class of antibiotics [6,7], has shown therapeutic efficacy against multidrug-resistant

* Corresponding author at: University of Lausanne, Quartier UNIL-SORGE, Biophore Building, Department of Fundamental Microbiology, CH-1015 Lausanne, Switzerland.
E-mail address: gregory.resch@unil.ch (G. Resch).

https://doi.org/10.1016/j.jgar.2019.05.005

A. baumannii (MDRAB). However, several reports of breakthrough infections have warranted caution for its use against this pathogen [8–10]. Moreover, extensively drug-resistant *A. baumannii* (XDRAB) strains producing the New Delhi metallo-ß-lactamase, which confers resistance to all ß-lactams including last-resort carbapenems, have very recently emerged [11,12]; infected patients have increased mortality, morbidity and length of hospitalisation [13].

There is a worrying lack of new agents with new targets or mechanisms of action against MDR Gram-negative bacteria, and two such potential molecules were identified in the early stages of development in 2009 [14]. Therefore, the time has come for global commitment to develop new antibacterial drugs for treating MDR Gram-negative-associated infections, and MDRAB-associated infections in particular. Accordingly, several preventive and therapeutic strategies have been considered, amongst which is the promising phage therapy approach [15]. The current study characterised two newly isolated bacteriophages against *A. baumannii* and assessed their activity in vitro and in vivo in *Galleria mellonella* and in a mouse model of bacteraemia. Their remarkable efficacy either as mono-therapy or in combination compared with imipenem in the mouse model combined with optimal in silico safety profiles suggest that these phages could be developed as alternatives for the treatment of *A. baumannii*-invasive infections.

2. Materials and methods

2.1. Bacterial strains and growth conditions

The OXA-23 and AmpC multidrug-resistant *A. baumannii* strain FER (FER), kindly provided by Patrice Nordmann, was chosen for the in vivo experiments [16]. In addition, 82 *A. baumannii* clinical isolates collected at the University hospital of Lausanne were obtained from the Institute of microbiology of the University of Lausanne and investigated (Table S1). The 83 isolates were grown in Luria Broth (LB) at 37 °C and 200 rpm for 16 h and on LB agar plates aerobically at 37 °C for 24 h.

2.2. Antibiotic susceptibility

The *A. baumannii* strain collection was provided with antibiograms previously determined using the Vitek-2 apparatus with AST-N420 card (Biomérieux SA, Marcy l'Etoile, France) and interpreted according to the most recent European Committee on Antimicrobial Susceptibility Testing clinical breakpoints (Table S1) [17].

2.3. Isolation of bacteriophages

Phages were amplified from samples of 12.5 mL raw sewage water (Vidy wastewater treatment plant, Lausanne, Switzerland) mixed with 1.5 mL of LB 10X and 1 mL of an overnight (o/n) culture of strain FER. After 24 h at 37 °C and 200 rpm, the amplification mixture was centrifuged at 4000 g for 15 min. Supernatant was filtered through 0.45 μm syringe filters (Cobetter Lab, Hangzhou, China) and stored at 4 °C until further use. Supernatant was further investigated through double-layer assays to obtain individual plaque-forming units (PFU). Briefly, 0.2 mL of bacterial o/n culture and 0.1 mL serial dilution of supernatant were mixed in 4 mL LB-soft agar and poured on top of LB agar plates. Individuals PFU were picked and mixed in 5 mL LB supplemented with 250 μL of an o/n culture of FER. After 24 h at 37 °C, the mixture was centrifuged at 4000 rpm for 15 min and filter sterilised through 0.22 μm syringe filters. The filtrate was processed through double-layer assay, as described above, and a second PFU was picked. The procedure was repeated at least three times to ensure selection of individual phages, which were stored at 4 °C until further use.

2.4. Determination of host ranges

Each phage was tested on each *A. baumannii* strain of the collection using classical drop test assay. Briefly, a strain was poured in a layer of soft agar and 5 μL drops of phage preparations were deposited on top of the solidified layer. After 24 h of incubation at 37 °C, plates were read by eye and lysis zones scored CL (Clear Lysis), SCL (Semi-Clear Lysis) or OL (Opaque Lysis). For FER, which was chosen for the in vivo tests, serial dilutions of stock solution were deposited in order to check for infectivity.

2.5. Phage adsorption

Exponentially growing *A. baumannii* FER (10^8 CFU/mL) were mixed with corresponding phages at MOI of 1 and incubated at 37 °C in a water bath; 100 μL of the mixture was collected every 5 min for 60 min and diluted 100 times in LB supplemented with 4% (vol/vol) chloroform. For each tube, phage titre was determined through double-layer assay using *A. baumannii* FER as the host strain. The rate of adsorption was calculated accordingly. Experiments were performed in triplicate.

2.6. Electron microscopy

Morphology of phage particles was studied using a JEOL 100C electron microscope (Jeol, Akishima-Shi, Tokyo, Japan). Phage suspension (10^9–10^{10} PFU/mL) was transferred onto carbon-coated copper grids for 30 s to let particles settle, and stained with 1% uranyl-acetate for 40 s. Filter paper was used to wick away excess sample. Grids were examined at different magnifications.

2.7. Full genome sequencing and analysis

Phage genomic DNA was extracted and purified using a classical phenol/chloroform extraction method [18].

2.8. Illumina sequencing and reads assembly

The vB_AbaM_3054 genomic DNA fragment sequencing libraries were prepared using the TruSeq Nano DNA LT Library Preparation Kit (Illumina, San Diego, USA) according to the supplied protocol and using 200 ng of genomic DNA. The resulting library was 100 nt paired-end sequenced on the Illumina HiSeq 2500 using TruSeq PE Cluster Kit v4 reagents and TruSeq SBS Kit v4 reagents. Sequencing data were processed using the Illumina Pipeline Software version 1.84. After adapter trimming using trimmomatic-0.36, assembly was automatically performed using spades [19].

2.9. PacBio sequencing and assembly

Genomic DNA of phage vB_AbaM_3090 was sequenced through Pacific Bioscience (PacBio) sequencing. The DNA was sheared in a Covaris g-TUBE (Covaris, Woburn, MA, USA) to obtain 20 kb fragments. After shearing, the DNA size distribution was checked on a fragment analyser (Advanced Analytical Technologies, Ames, IA, USA). Then, 1.3 μg of the sheared DNA was used to prepare a SMRTbell library with the PacBio SMRTbell Template Prep Kit 1 (Pacific Biosciences, Menlo Park, CA, USA) according to the manufacturer's recommendations. The library was sequenced on one SMRT cell with P6/C4 chemistry and MagBeads on a PacBio RSII system (Pacific Biosciences, Menlo Park, CA, USA) at 240-min movie length. The PacBio module RS_HGAP_Assembly.2 in SMRTpipe version v2.3.0 was used to assemble the obtained reads.

2.10. Genome annotation

Open reading frames (ORF, minimum size of 100 amino acids) and tRNA encoding genes were identified on phage genomes and annotated using ORF Finder [20] and Prokka [21]. In addition, phage genomic sequences were checked for gene coding virulence factors and antibiotic resistance using the blast interface of the Virulence Factors of Pathogenic Bacteria database (www.mgc.ac.cn/VFs) and the ResFinder tool from the Center for Genomic Epidemiology (https://cge.cbs.dtu.dk//services/ResFinder), respectively.

2.11. In vitro turbidity assays in 96-well plates

FER was grown in 10 mL LB at 37 °C and 200 rpm for 16 h. After centrifugation of the culture at RT and 4000 rpm for 20 min, the bacterial pellet was thoroughly resuspended in 50 mL saline. Then, 10 μL of this bacterial suspension (i.e. 10^6 CFU) were mixed in 96-well plates with 10 μL of phage suspensions at different concentrations (i.e. 10^4, 10^6 and 10^8 PFU) or 10 μL of imipenem at 5 mg/mL (final concentration of 167 μg/mL) and 280 μL LB. The microtiter plate was placed in a microplate reader set at 37 °C and first measurement at OD_{600nm} was taken immediately. Additional measurements were taken every 10 min for 24 h. The microplate was shacked for 3 s before each measurement. All experiments were performed in triplicate.

2.12. Acinetobacter baumannii *experimental bacteraemia in* Galleria mellonella

Wax moths (n = 18) were challenged in the last right pseudopod with 5.10^5 CFU of FER in 5 μL saline. Phages (5.10^7 PFU in 10 μL saline; MOI = 100) were administrated in the last left pseudopod, alone or in combination, by a single bolus injection 30 min after bacterial challenge. Saline and imipenem at 5 mg/mL were injected as controls. The survival rates of larvae were followed over a period of 80 h and compared with Log-Rank (Mantel-Cox) and Gehan-Breslow-Wilcoxon tests using GraphPad Prism version 5.00 for Windows (GraphPad Software, San Diego, CA, USA, www.graphpad.com).

2.13. Acinetobacter baumannii *experimental bacteraemia in mice*

The mice model of bacteraemia was carried out in strict accordance with the recommendations of the Swiss Federal Act on Animal Protection. The protocol was approved by the Committee on the Ethics of Animal Experiments of the Consumer and Veterinary Affairs Department of the State of Vaud (Permit No 3065). A total of 30 CD1 Swiss female mice (Charles River Laboratories, L'Arbresle, France), with an average weight of 21 ± 1 g, were used in this study. The animal sample size (n) was estimated to be six with the formula for dichotomous variables (expected pc = 1 and pe = 0.2; with pc = death event in control group, pe = death event in experimental group and C = 7.85) [22]. In order to induce bacteraemia, the mice were intraperitoneally (i.p.) challenged with 6.10^7 CFU of FER in 100 μL saline. Bacteraemia state at the time of the initial treatment injection was validated after aseptic removal of the left kidney and spleen from three mice 2 h after i.p injection of 6.10^7 CFU of FER in 100 μL saline. Organs were homogenised in 1 mL of saline and briefly centrifuged, and supernatants were plated on blood agar plates to determine the number of viable organisms in tissues. Phages (6.10^9 PFU in 200 μL saline; MOI of 100) were administrated i.p. alone or in combination by a single bolus injection 2 h after bacterial challenge; 200 μL saline and 200 μL imipenem at 5 mg/mL (ca. 50 mg/kg) were injected as controls. The survival rates of animals were followed over a period of 7 days and compared with Log-Rank (Mantel-Cox) and Gehan-Breslow-Wilcoxon tests using GraphPad Prism version 5.00 for Windows.

3. Results

3.1. Isolation and characterisation of Acinetobacter baumannii phages

Two phages – named vB_AbaM_3054 and vB_AbaM_3090 – were successfully isolated through classical amplification from samples of wastewater. Phage vB_AbaM_3054 formed small clear plaques surrounded by halos, and phage vB_AbaM_3090 formed tiny clear plaques with no halo on a lawn of FER (Fig. S1).

3.2. Phage host range and adsorption rate

The host range of both phages was quickly screened by drop test on the collection of 83 clinical isolates (Table S2). Both phages were very strain-specific, with CL or SCL lysis on 10.8% and 14.5% of the tested strains (Table S2). In addition, since FER was chosen for the in vivo study, infectivity of both phages was checked by drop tests of serially diluted stock solutions (non-diluted to 10^8 dilutions). As shown in Fig. S2, both phages formed well-separated plaques on FER at high dilutions (i.e. up to 10^8 and up to 10^4 for vB_AbaM_3054 and vB_AbaM_3090, respectively) confirming infectivity of both phages on FER. Examination of phage particle morphology by TEM revealed that both phages belonged to the Myoviridae family. The size of vB_AbaM_3054 head was 102 × 94 nm and the size of the tail 88 × 22 nm (Fig. 1A). The size of vB_AbaM_3090 head was 113 × 108 nm and the size of the tail 130 × 13 nm (Fig. 1B). The adsorption rate was 89 ± 4% and 95 ± 2% in 10 min for vB_AbaM_3054 and vB_AbaM_3090, respectively.

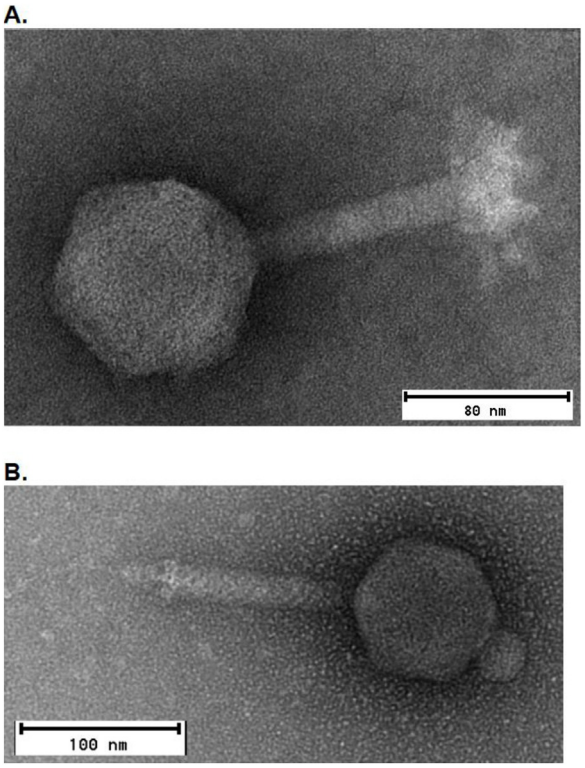

Fig. 1. Electronic microscopy micrographs of phages.
A. vB_AbaM_3054; scale bar represents 80 nm.
B. vB_AbaM_3090; scale bar represents 100 nm.
Morphology of phage particles was studied using a JEOL 100C electron microscope (Jeol, Akishima-Shi, Tokyo, Japan).

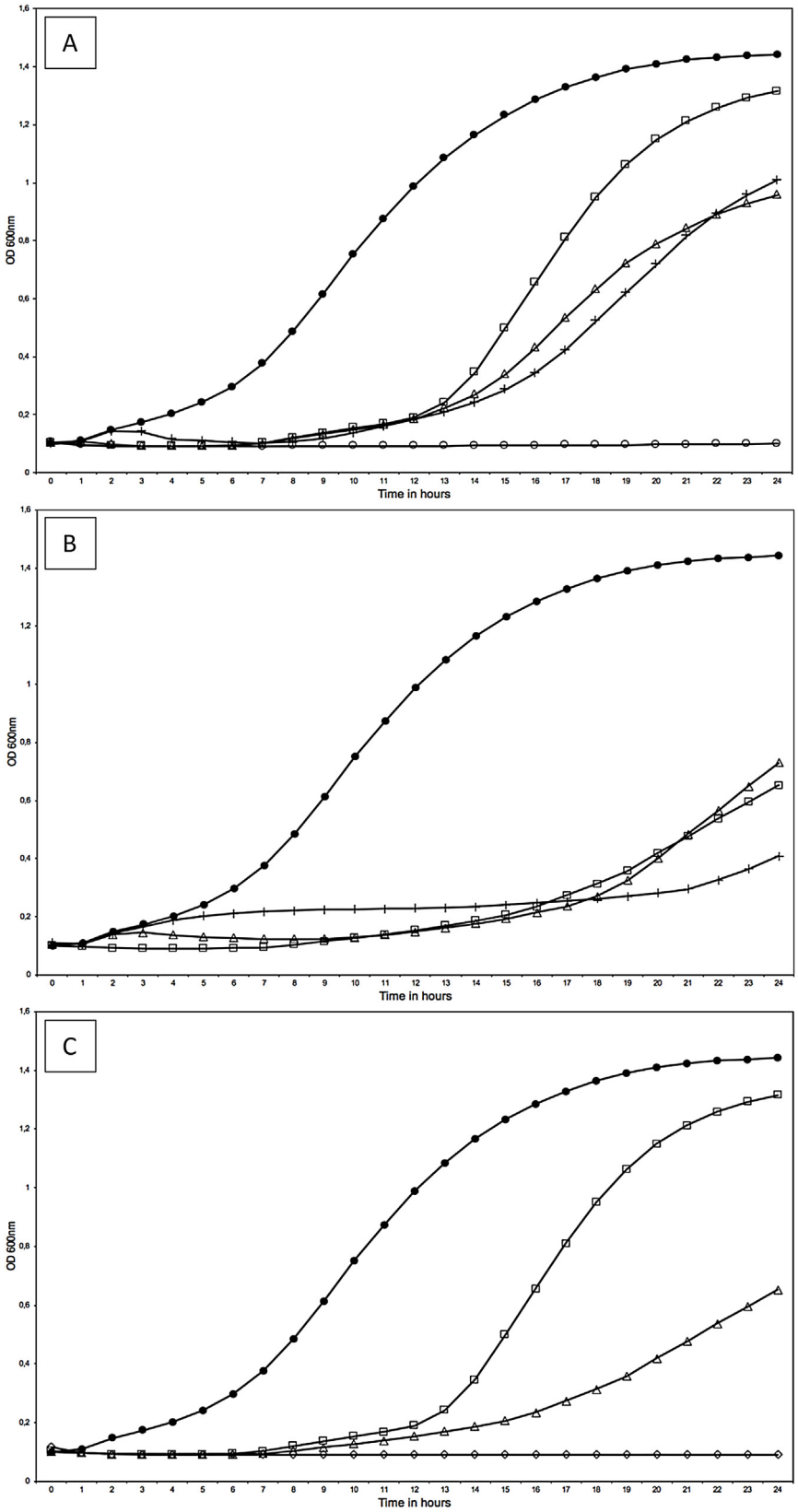

Fig. 2. Effect of different treatments on the growth of *A. baumannii* strain FER in a 96-well plate turbidity assay.
OD_{600nm} was recorded every 10 min over 24 h. For clarity, only one measurement per hour is indicated.
A. vB_AbaM_3054 at different MOI and imipenem. Control (NaCl, filled circles); vB_AbaM_3054 (MOI of 100, open squares); vB_AbaM_3054 (MOI of 1, open triangles); vB_AbaM_3054 (MOI of 0.01, crosses); imipenem (167 μg/mL, open circles).
B. vB_AbaM_3090 at different MOI. Control (NaCl, filled circles); vB_AbaM_3090 (MOI of 100, open squares); vB_AbaM_3090 (MOI of 1, open triangles); vB_AbaM_3090 (MOI of 0.01, crosses).
C. vB_AbaM_3054 and vB_AbaM_3090 at MOI of 100 alone or in combination. Control (NaCl, filled circles); vB_AbaM_3054 (MOI of 100, open squares); vB_AbaM_3090 (MOI of 100, open triangles); vB_AbaM_3054 + vB_AbaM_3090 (MOI of 50 each, open diamonds). Each dot represents the mean of three independent experiments.

3.3. Phage genome sequencing and analysis

Both phages harboured a double-stranded DNA genome successfully purified by classical phenol/chloroform extraction.

3.3.1. vB_AbaM_3054

Sequencing of the genome of vB_AbaM_3054 through Illumina 100 bp paired-end sequencing yielded a draft genome consisting of four contigs of 16549 bp (vB_AbaM_3054_contig1), 14254 bp (vB_AbaM_3054_contig2), 13184 bp (vB_AbaM_3054_contig3) and 5456 bp (vB_AbaM_3054_contig4) for a total length of 49443 bp. As listed in Table S3, blastn against the 'nr' database identified very few homologies with already published sequences of phage vB_AbaP_B1 (Genbank accession No MF033347.1) and phage SH-Ab 15599 (Genbank accession No MH517022.1). A detailed analysis revealed presence of 47 ORFs of >100 amino acids (aa) on the draft genome, amongst which 14 matched phage proteins using blastp against the 'non-redundant protein sequences (nr)' database. While two structural genes (i.e. tail fibre proteins) were identified on vB_AbaM_3054_contig1, ORFs possibly involved in replication (DNA ligase, hydrolase, DNA topoisomerase and exonuclease) were identified on the three other contigs. ORF7 on vB_AbaM_3054_contig4 encoded for a protein showing significant homology with several cell wall hydrolases and likely corresponded to the lysin of vB_AbaM_3054.

3.3.2. vB_AbaM_3090

Sequencing of vB_AbaM_3090 through PacBio technology yielded a single contig of 104796 bp. Blastn identified vB_AbaM_phiAbaA1 (GenBank accession No KJ628499) as a very close neighbour with 98% identity over 98% query coverage. A total of 166 ORFs and 13 tRNA genes were identified on vB_AbaM_3090 genome; 157 ORFs were assigned 'hypothetical proteins' (not shown).

3.4. Minimum inhibitory concentration and in vitro turbidity assays

The MIC of imipenem was 32 mg/L for FER (not shown). The effects of the different treatments on the in vitro bacterial growth are presented in Fig. 2. For clarity of the graphics, hourly measurements are reported in the figures. vB_AbaM_3054 showed very similar patterns of bacterial growth inhibition independent to the MOI (range 0.01–100), except that the initial bacterial growth at 1 h was progressively inhibited with full inhibition at MOI of 100 (Fig. 2A, open squares). Of note, a secondary bacterial regrowth starting at ca. 7 h was observed at all MOI (Fig. 2A). Bacterial growth inhibition by vB_AbaM_3090 followed very similar patterns at the three different MOIs and the initial bacterial growth was also fully inhibited at a MOI of 100 (Fig. 2B, open squares). As for vB_AbaM_3054, the secondary growth started at ca. 7 h but followed a less steep slope (Fig. 2B and C). In view of these first results with monophage preparations, an MOI of 100 was considered for the in vivo models. Therefore, a combination of both phages at this MOI was further tested in vitro. As seen in Fig. 2C, the combination of both phages at an MOI of 100 was highly synergistic and fully prevented secondary growth for up to 24 h (Fig. 2C, open diamonds). Similar results were observed in vitro with imipenem at the high dose of 5 mg/mL (>5 times the MIC), a concentration mimicking recommended in vivo dosage (for convenience only reported in Fig. 2A, open circles).

3.5. Therapeutic efficacy in a Galleria mellonella model of A. baumannii infection

Efficacy of both phages at an MOI of 100, either alone or in combination, was further compared with a single bolus injection of the standard of care imipenem on the survival of *Galleria mellonella* challenged with ca. 5.10^5 CFU of *A. baumannii* FER (Fig. 3). This bacterial inoculum led to 0% survival of the wax moths at 48 h in the untreated control group. When injected 30 min after bacterial challenge, all treatments led to significantly improved survival at 80 h ($P < 0.001$ compared with the untreated control for all treatments) and the effect was not significantly different between the treatments (100%, ca. 83%, ca. 89% and ca. 95% survival at 80 h for vB_AbaM_3054, vB_AbaM_3090, combination of both phages and imipenem, respectively; $P = 0.32$).

3.6. Therapeutic efficacy in a mouse model of A. baumannii bacteraemia

Three mice were challenged i.p. with 6.10^7 CFU of FER in 100 µL saline. Animals were euthanised 2 h after infection and organs were homogenised and tested for the presence of viable bacteria. A total of $>10^5$ CFU/g were found in the spleen and kidney (data not shown), demonstrating infection dissemination and the bacteraemic state of the mice at this time point. Efficacy of both phages at an MOI of 100, either alone or in combination, was further compared with a single bolus injection of imipenem on the survival of mice challenged i.p. with ca. 6.10^7CFU of FER (n = 6, Fig. 4). According to the bacteraemic state previously demonstrated, this bacterial inoculum led to 0% survival of the animals at day 1 in the untreated control group. Phage treatments injected 2 h after infection led to improved survival at day 7 ($P < 0.001$, compared with the untreated control for all phage treatments) and the effect was not significantly different between treatments (80%, 100% and 80%, for vB_AbaM_3054, vB_AbaM_3090 and the combination of both phages, respectively; $P = 0.59$). In contrast, with ca. 17% survival at day 7, a single bolus injection of 50 mg/kg imipenem failed to rescue the mice ($P = 0.32$ compared with the untreated control).

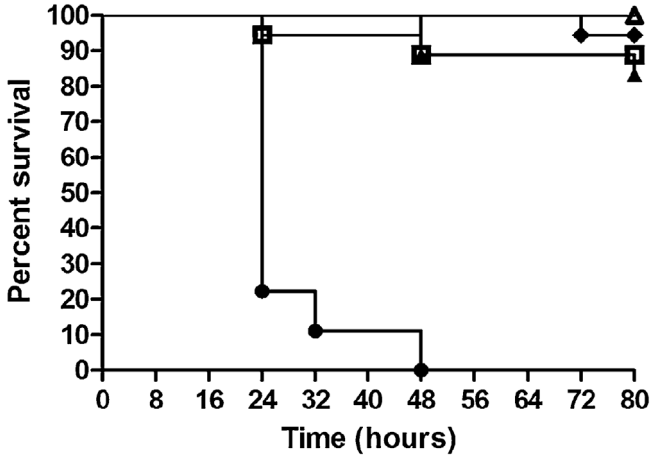

Fig. 3. Efficacy of phage therapy in a *Galleria mellonella* model of *A. baumannii* bacteraemia.
Wax moths (n = 18) were injected in the last right pseudopod with 5.10^5 CFU *A. baumannii* FER. They received, in the left pseudopod, NaCl (control, closed circles), vB_AbaM_3054 (MOI of 100, open triangles), vB_AbaM_3090 (MOI of 100, closed triangles), vB_AbaM_3054 + vB_AbaM_3090 (MOI of 50 each, open squares) or imipenem (5 mg/mL, closed diamonds) 30 min later. Larvae were monitored for survival over a period of 80 h and results were plotted as Kaplan-Meier survival curves. Curves were compared with the log-rank (Mantel-Cox) and Gehan-Breslow-Wilcoxon tests. All treatments groups were significantly different compared with the untreated control group ($P < 0.001$). There were no statistically significant differences between treatments ($P = 0.32$).

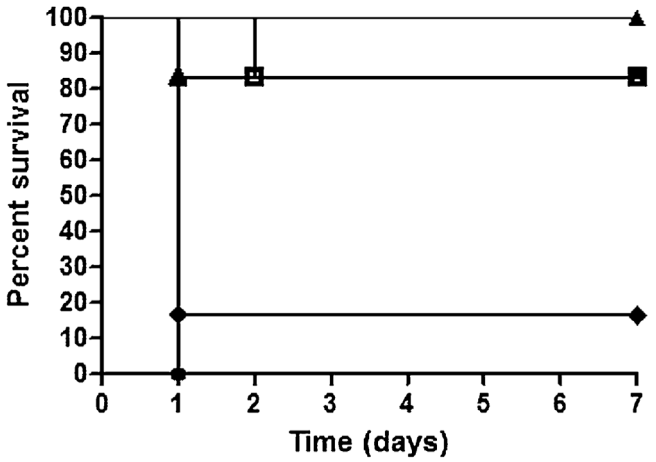

Fig. 4. Efficacy of phage therapy in a mouse model of *A. baumannii* bacteraemia. CD1 Swiss mice (n = 6) were injected i.p. with ca. 6.10^7 CFU of *A. baumannii* FER. At 2 h post infection, animals received an intraperitoneal injection of NaCl (control, closed circles), vB_AbaM_3054 (MOI of 100, open triangles), vB_AbaM_3090 (MOI of 100, closed triangles), vB_AbaM_3054 + vB_AbaM_3090 (MOI of 50 each, open squares) or imipenem (5 mg/mL ≈50 mg/kg, closed diamonds). Mice were monitored for survival over a period of 7 days and results were plotted as Kaplan-Meier survival curves. Survival curves were compared with the log-rank (Mantel-Cox) and Gehan-Breslow-Wilcoxon tests. All phage treatments groups were significantly different compared with the untreated control group ($P < 0.001$). There were no statistically significant differences between phage treatments ($P = 0.59$). Imipenem group was not statistically significantly different to the untreated control group ($P = 0.32$).

4. Discussion

Bacteraemia is one of the most significant infections caused by *A. baumannii*. Its clinical manifestations range from transient bacteraemia to septic shock with high mortality [23]. Phage therapy has been documented on multiple occasions as a promising alternative to treat *A. baumannii* infections. Indeed, the therapeutic potential of anti-*A. baumannii* phages has been demonstrated since 2015 but mainly in rodent models of wound [24–26] and lung [27–29] infections. Interestingly, a very recent human case report demonstrated efficacy of phage therapy (as adjunct to antibiotherapy) in a patient suffering from a disseminated resistant *A. baumannii* infection [30].Of note, it has also recently been shown that strategies using prophage-derived lysin or derived peptides can rescue mice from otherwise lethal *A. baumannii*-induced bacteraemia [31,32]. Accordingly, the current study aimed to evaluate the therapeutic potential of phages in a mouse model of bacteraemia. Following efforts to isolate lytic *A. baumannii* phages, it focused more closely on two very potent candidates belonging to the Myoviridae family, namely vB_AbaM_3054 and vB_AbaM_3090, harbouring strong in vitro lytic activity against the *A. baumannii* clinical strain FER, representative of the commonly encountered serotype 2. The clinical relevance of this strain has previously been shown when it was found to harbour a plasmid (pFER) carrying a $bla_{OXA\text{-}23}$ gene conferring higher levels of carbapenem resistance than the one conferred by the recombinant plasmid pOXA-23 or pOXA-58 [16].

Full genome sequencing of both phages has revealed their potential to be considered as antibacterial agents administrable to humans, since neither virulence nor resistance genes could have been detected [33]. In addition, the absence of integrase genes argues for strict lytic lifestyle of both phages. Taken together, these data consolidated their potential safety. In vitro tests revealed the therapeutic potential of the two phages, which were both able to dramatically inhibit growth of FER in turbidity assays at low (0.01), medium (1) and high (100) MOI. The curve profiles were highly similar at the different MOIs, except that the initial bursts of bacterial growth, which occurred at low MOIs and were totally inhibited at a high MOI of 100. Of note, in all conditions, bacterial regrowth was observed after 7 h, which was likely due to the selection of phage-resistant bacterial variants, as often observed in vitro. *A. baumannii* FER was confirmed to be resistant to imipenem with an MIC of 32 mg/L and it was therefore unsurprising that this carbapenem performed very well in vitro at a concentration of 167 μg/mL (i.e. > 5 times the MIC of 32 mg/L) with no detectable bacterial growth over 24 h.

In vitro efficacy results for phages at MOI 100 and imipenem transposed to *Galleria mellonella*. Indeed, both treatments achieved high protection in wax moths with ca. 100% survival at 80 h post-infection. Interestingly, *Galleria mellonella* successfully predicted the outcome of phage therapy in mice in which all phage-based treatments achieved ca. 100% survival rate 7 days after the bacterial challenge. This observation agreed with previous studies reporting *Galleria mellonella* as a useful pre-screening model for evaluating phages as antimicrobials before testing in more sophisticated mammalian models [34,35]. However, imipenem 5 mg/mL rescued 95% of the *Galleria mellonella* and therefore failed to predict the outcome in mice, in which it was inactive. This discrepancy might be explained by a bioavailability of imipenem in *Galleria mellonella* similar to the test tube situation and/or differences in the immune systems in comparison with mice [36]. Therefore, this result poses the question of whether *Galleria mellonella* is a relevant in vivo model in this setting.

Contrasting in vitro results (i.e. secondary growth) with high in vivo potencies of monophage preparations question the clinical relevance of potential phage-resistant mutants selected in vitro. Additional experiments are needed to fully characterise the selected mutants in order to determine whether the observed discrepancies could be explained by a high fitness cost leading to the incapacity of the mutants selected in vitro to survive or infect in vivo, as recently reported in other bacterial species [37,38].

Bearing in mind all the remaining challenges and unanswered questions, the current authors are convinced that these data showing efficacy of phage therapy in a mouse model of XDRAB bacteraemia could pave the way for developing phage therapy to manage systemic infections due to MDRAB and XRDAB.

Funding

This work was supported by a SCOPES grant (No IZ07Z0_160907) from the SNFSR to G.R. The Pacific Biosciences RSII instrument was financed in part by the Loterie Romande.

Competing interests

The authors declare that they have no competing interests.

Ethical approval

The protocol was approved by the Committee on the Ethics of Animal

Experiments of the Consumer and Veterinary Affairs Department of the State of Vaud (authorisation No 3065).

Acknowledgments

We are particularly thankful to Patrice Nordmann for kindly providing us with the *A. baumannii* strain FER. We thank Aurélie Marchet, Julie Luche and Jean Daraspe for excellent technical assistance.

Appendix A. Supplementary data

Supplementary material related to this article can be found, in the online version, at doi:https://doi.org/10.1016/j.jgar.2019.05.005.

References

[1] Seifert H, et al. Distribution of Acinetobacter species on human skin: comparison of phenotypic and genotypic identification methods. J Clin Microbiol 1997;35:2819–25.
[2] Visca P, Seifert H, Towner KJ. Acinetobacter infection—an emerging threat to human health. IUBMB Life 2011;63:1048–54, doi:http://dx.doi.org/10.1002/iub.534.
[3] Rice LB. Federal funding for the study of antimicrobial resistance in nosocomial pathogens: no ESKAPE. J Infect Dis 2008;197:1079–81, doi:http://dx.doi.org/10.1086/533452.
[4] Rice LB. Progress and challenges in implementing the research on ESKAPE pathogens. Infect Control Hosp Epidemiol 2010;31 Suppl 1:S7–10, doi:http://dx.doi.org/10.1086/655995.
[5] Koulenti D, et al. Spectrum of practice in the diagnosis of nosocomial pneumonia in patients requiring mechanical ventilation in European intensive care units. Crit Care Med 2009;37:2360–8, doi:http://dx.doi.org/10.1097/CCM.0b013e3181a037ac.
[6] Rose WE, Rybak MJ. Tigecycline: first of a new class of antimicrobial agents. Pharmacotherapy 2006;26:1099–110, doi:http://dx.doi.org/10.1592/phco.26.8.1099.
[7] Kasbekar N. Tigecycline: a new glycylcycline antimicrobial agent. Am J Health Syst Pharm 2006;63:1235–43, doi:http://dx.doi.org/10.2146/ajhp050487.
[8] Peleg AY, et al. *Acinetobacter baumannii* bloodstream infection while receiving tigecycline: a cautionary report. J Antimicrob Chemother 2007;59:128–31, doi:http://dx.doi.org/10.1093/jac/dkl441.
[9] Peleg AY, Adams J, Paterson DL. Tigecycline efflux as a mechanism for nonsusceptibility in *Acinetobacter baumannii*. Antimicrob Agents Chemother 2007;51:2065–9, doi:http://dx.doi.org/10.1128/AAC.01198-06.
[10] Shin JA, et al. Clinical outcomes of tigecycline in the treatment of multidrug-resistant *Acinetobacter baumannii* infection. Yonsei Med J 2012;53:974–84, doi:http://dx.doi.org/10.3349/ymj.2012.53.5.974.
[11] Chen Y, Zhou Z, Jiang Y, Yu Y. Emergence of NDM-1-producing *Acinetobacter baumannii* in China. J Antimicrob Chemother 2011;66:1255–9, doi:http://dx.doi.org/10.1093/jac/dkr082.
[12] Sowmiya M, Umashankar V, Muthukumaran S, Madhavan HN, Malathi J. Studies on New Delhi metallo-beta-lactamse-1 producing *Acinetobacter baumannii* isolated from donor swab in a tertiary eye care centre, India and structural analysis of its antibiotic binding interactions. Bioinformation 2012;8:445–52, doi:http://dx.doi.org/10.6026/97320630008445.
[13] Maragakis LL, Perl TM. *Acinetobacter baumannii*: epidemiology, antimicrobial resistance, and treatment options. Clin Infect Dis 2008;46:1254–63, doi:http://dx.doi.org/10.1086/529198.
[14] Boucher HW, et al. 10 x' 20 progress—development of new drugs active against gram-negative bacilli: an update from the Infectious Diseases Society of America. Clin Infect Dis 2013;56:1685–94, doi:http://dx.doi.org/10.1093/cid/cit152.
[15] Garcia-Quintanilla M, Pulido MR, Lopez-Rojas R, Pachon J, McConnell MJ. Emerging therapies for multidrug resistant *Acinetobacter baumannii*. Trends Microbiol 2013;21:157–63, doi:http://dx.doi.org/10.1016/j.tim.2012.12.002.
[16] Heritier C, Poirel L, Lambert T, Nordmann P. Contribution of acquired carbapenem-hydrolyzing oxacillinases to carbapenem resistance in *Acinetobacter baumannii*. Antimicrob Agents Chemother 2005;49:3198–202, doi:http://dx.doi.org/10.1128/AAC.49.8.3198-3202.2005.
[17] The European Committee on Antimicrobial Susceptibility Testing. Breakpoint tables for interpretation of MICs and zone diameters. Version 8.1. 2018.
[18] Sambrook J, Fritsch EF, Maniatis T. Molecular cloning: a laboratory manual. 2nd ed. New York: Cold Spring Harbor Laboratory Press; 1989.
[19] Bankevich A, et al. SPAdes: a new genome assembly algorithm and its applications to single-cell sequencing. J Comput Biol 2012;19:455–77, doi:http://dx.doi.org/10.1089/cmb.2012.0021.
[20] ORF Finder 2015. http://www.ncbi.nlm.nih.gov/gorf/orfig.cgi. [Accessed 8 May]
[21] Seemann T. Prokka: rapid prokaryotic genome annotation. Bioinformatics 2014;30:2068–9, doi:http://dx.doi.org/10.1093/bioinformatics/btu153.
[22] Shah H. How to calculate sample size in animal studies? Natl J Physiol Pharm Pharmacol 2011;1:35–9.
[23] Cisneros JM, et al. Bacteremia due to *Acinetobacter baumannii*: epidemiology, clinical findings, and prognostic features. Clin Infect Dis 1996;22:1026–32.
[24] Yin S, et al. Phage Abp1 rescues human cells and mice from infection by pan-drug resistant *Acinetobacter baumannii*. Cell Physiol Biochem 2017;44:2337–45, doi:http://dx.doi.org/10.1159/000486117.
[25] Kusradze I, et al. Characterization and testing the efficiency of *Acinetobacter baumannii* phage vB-GEC_Ab-M-G7 as an antibacterial agent. Front Microbiol 2016;7:1590, doi:http://dx.doi.org/10.3389/fmicb.2016.01590.
[26] Regeimbal JM, et al. Personalized therapeutic cocktail of wild environmental phages rescues mice from *Acinetobacter baumannii* wound infections. Antimicrob Agents Chemother 2016;60:5806–16, doi:http://dx.doi.org/10.1128/AAC.02877-15.
[27] Jeon J, et al. In vivo application of bacteriophage as a potential therapeutic agent to control OXA-66-like carbapenemase-producing *Acinetobacter baumannii* strains belonging to sequence type 357. Appl Environ Microbiol 2016;82:4200–8, doi:http://dx.doi.org/10.1128/AEM.00526-16.
[28] Wang Y, et al. Intranasal treatment with bacteriophage rescues mice from *Acinetobacter baumannii*-mediated pneumonia. Future Microbiol 2016;11:631–41, doi:http://dx.doi.org/10.2217/fmb.16.11.
[29] Shivaswamy VC, et al. Ability of bacteriophage in resolving wound infection caused by multidrug-resistant *Acinetobacter baumannii* in uncontrolled diabetic rats. Microb Drug Res 2015;21:171–7, doi:http://dx.doi.org/10.1089/mdr.2014.0120.
[30] Schooley RT, et al. Development and use of personalized bacteriophage-based therapeutic cocktails to treat a patient with a disseminated resistant *Acinetobacter baumannii* infection. Antimicrob Agents Chemother 2017;61:, doi:http://dx.doi.org/10.1128/AAC.00954-17.
[31] Lood R, et al. Novel phage lysin capable of killing the multidrug-resistant gram-negative bacterium *Acinetobacter baumannii* in a mouse bacteremia model. Antimicrob Agents Chemother 2015;lume-nr>1983–91, doi:http://dx.doi.org/10.1128/AAC.04641-14.
[32] Peng SY, et al. Highly potent antimicrobial modified peptides derived from the *Acinetobacter baumannii* phage endolysin LysAB2. Sci Rep 2017;7:11477, doi:http://dx.doi.org/10.1038/s41598-017-11832-7.
[33] Pirnay JP, et al. Quality and safety requirements for sustainable phage therapy products. Pharm Res 2015;32:2173–9, doi:http://dx.doi.org/10.1007/s11095-014-1617-7.
[34] Abbasifar R, et al. Efficiency of bacteriophage therapy against *Cronobacter sakazakii* in *Galleria mellonella* (greater wax moth) larvae. Arch Virol 2014;159:2253–61, doi:http://dx.doi.org/10.1007/s00705-014-2055-x.
[35] Beeton ML, Alves DR, Enright MC, Jenkins AT. Assessing phage therapy against *Pseudomonas aeruginosa* using a *Galleria mellonella* infection model. Int J Antimicrob Agents 2015;46:196–200, doi:http://dx.doi.org/10.1016/j.ijantimicag.2015.04.005.
[36] Tsai CJ, Loh JM, Proft T. *Galleria mellonella* infection models for the study of bacterial diseases and for antimicrobial drug testing. Virulence 2016;7:214–29, doi:http://dx.doi.org/10.1080/21505594.2015.1135289.
[37] Oechslin F, et al. Synergistic interaction between phage therapy and antibiotics clears *Pseudomonas aeruginosa* infection in endocarditis and reduces virulence. J Infect Dis 2017;215:703–12, doi:http://dx.doi.org/10.1093/infdis/jiw632.
[38] Leon M, Bastias R. Virulence reduction in bacteriophage resistant bacteria. Front Microbiol 2015;6:343, doi:http://dx.doi.org/10.3389/fmicb.2015.00343.